

Open-file 78-591

Open-file 78-591

UNITED STATES
DEPARTMENT OF THE INTERIOR
GEOLOGICAL SURVEY

THE UTILITY OF PETROLEUM SEISMIC EXPLORATION
DATA IN DELINEATING STRUCTURAL FEATURES
WITHIN SALT ANTICLINES

By

S. L. Stockton and A. H. Balch

78-591

CONTENTS

	Page
Abstract-----	1
Introduction-----	2
Regional geologic setting-----	2
Stratigraphic framework and associated acoustic properties-----	4
Investigative procedures-----	4
Seismic field parameters-----	4
Seismic data processing-----	12
Interpretation of seismic data-----	18
Structural framework-----	18
Computer subsurface modeling-----	22
Recommendations-----	34
Vertical seismic profiling-----	34
Surface seismic methods-----	34
Borehole geophysics-----	35
Conclusions-----	35
References cited-----	36

ILLUSTRATIONS

	Page
Figure 1.--Map showing the approximate limits of the Paradox Basin and the outline of the Salt Valley anticline study area, Grand County, Utah-----	3
2.--Location of seismic profile line C over Salt Valley anticline-----	6
3.--Multifold, common-depth-point seismic section along profile line A-----	7
4.--Multifold, common-depth-point seismic section along profile line B-----	8
5. Multifold, common-depth-point seismic section along profile line C-----	10
6.--Structure contours on top of salt of the Paradox Member of the Hermosa Formation in the Salt Valley anticline-----	11
7.--Flow chart of the Paradox Basin data-processing sequence-----	13
8.--Frequency analyses-----	14
9.--Diffraction of seismic energy-----	15
10.--Migration of seismic events due to dipping beds-----	15
11.--Synthetic seismogram from an acoustic log-----	16
12.--Section B with synthetic seismogram from figure 11-----	17
13.--Section A. Lines show configuration of faults and salt-anticline units on flanks-----	19
14.--Section B. Lines show configuration of faults and salt-anticline units on flanks-----	20
15. Section C. Lines show configuration of faults and salt-anticline units on flanks-----	21

ILLUSTRATIONS--Continued

	Page
Figure 16.--Models of thin beds within salt showing thickness and velocity variations-----	23
17.--Synthetic seismic sections of thin beds-----	24
18.--Model of interbed in salt to observe the effect of the folding of thin beds in the seismic section-----	25
19.--Depth to seismic foci in buried and folded salt interbeds-----	26
20.--Model of a typical subsurface salt ridge derived from a composite of three seismic profiles, borehole information, and a hypothesis about the nature of the shallow faulting-----	27
21.--Normally incident ray paths generated for the subsurface model of figure 20-----	28
22.--Salt ridge and asymmetricly folded interbeds-----	29
23.--Synthetic seismic record section showing salt interbeds-----	30
24.--Synthetic salt-ridge seismic record section produced from the interbed reflections only-----	31
25.--Salt-ridge model with less complexly folded interbeds-----	32
26.--Less complex synthetic seismic record section showing interbed reflections only-----	33

TABLES

	Page
Table 1.--Paleozoic and Mesozoic stratigraphy and acoustic properties of the northwest Paradox Basin-----	5
2.--Summary of seismic field parameters-----	9

UNITED STATES
DEPARTMENT OF THE INTERIOR
GEOLOGICAL SURVEY

Mail Stop 954, Federal Center, Box 25046
Denver, Colorado 80225

THE UTILITY OF PETROLEUM SEISMIC EXPLORATION
DATA IN DELINEATING STRUCTURAL FEATURES
WITHIN SALT ANTICLINES

By

S. L. Stockton and A. H. Balch

ABSTRACT

The Salt Valley anticline, in the Paradox Basin of southeastern Utah, is under investigation for use as a location for storage of solid nuclear waste. Delineation of thin, nonsalt interbeds within the upper reaches of the salt body is extremely important because the nature and character of any such fluid- or gas-saturated horizons would be critical to the mode of emplacement of wastes into the structure.

Analysis of 50 km of conventional seismic-reflection data, in the vicinity of the anticline, indicates that mapping of thin beds at shallow depths may well be possible using a specially designed adaptation of state-of-the-art seismic oil-exploration procedures. Computer ray-trace modeling of thin beds in salt reveals that the frequency and spatial resolution required to map the details of interbeds at shallow depths (less than 750 m) may be on the order of 500 Hz, with surface-spread lengths of less than 350 m. Consideration should be given to the burial of sources and receivers in order to attenuate surface noise and to record the desired high frequencies.

Correlation of the seismic-reflection data with available well data and surface geology reveals the complex, structurally initiated diapir, whose upward flow was maintained by rapid contemporaneous deposition of continental clastic sediments on its flanks. Severe collapse faulting near the crests of these structures has distorted the seismic response. Evidence exists, however, that intrasalt thin beds of anhydrite, dolomite, and black shale are mappable on seismic record sections either as short, discontinuous reflected events or as amplitude anomalies that result from focusing of the reflected seismic energy by the thin beds; computer modeling of the folded interbeds confirms both of these as possible causes of seismic response from within the salt diapir. Prediction of the seismic signatures of the interbeds can be made from computer-model studies.

Petroleum seismic-reflection data are unsatisfactory for mapping the thin beds because of the lack of sufficient resolution to provide direct evidence of the presence of the thin beds. However, indirect evidence, present in these data as discontinuous seismic events, suggests that two geophysical techniques designed for this specific problem would allow direct detection of the interbeds in salt. These techniques are vertical seismic profiling and shallow, short-offset, high-frequency, seismic-reflection recording.

INTRODUCTION

The Salt Valley anticline, a major linear salt diapir in the Paradox Basin of southeastern Utah (fig. 1), is currently under consideration by DOE (U.S. Department of Energy) as a possible location for the isolation of solid nuclear waste. The Salt Valley anticline is well qualified for further study as a potential waste emplacement site because it possesses certain favorable geologic characteristics and is readily accessible by land transportation.

Intensely deformed, thin (5-70 m) interbeds of anhydrite, dolomite, and black shale sometimes occur within the halite core. Some of these beds are known to contain water and hydrocarbons under high pressure. The major objective of this investigation was to determine whether the thin beds could be detected by using seismic-reflection data. Additional objectives were as follows:

1. The interpretation and correlation of existing seismic data, borehole data, and surface geology (fig. 2), and the analysis of the growth history of the Salt Valley anticline.
2. The determination of the minimum acceptable seismic resolution needed to detect thin beds and the determination of the maximum thickness detectable by conventional methods.
3. The isolation and identification of seismic signatures from thin beds in an otherwise homogeneous medium.
4. The proposal or recommendation for further studies, if appropriate.

Three multifold, 50-km-long seismic-reflection profiles, which were obtained from the petroleum industry, were extensively processed and interpreted. A subsurface ray-trace computer-modeling system was used to formulate hypothetical models of both the internal and external structure of a salt anticline. The resultant synthetic seismic sections were used to test the validity of the interpretation and to design a seismic technique especially tailored to the marker-bed problem.

REGIONAL GEOLOGIC SETTING

The Paradox Basin (fig. 1) covers approximately 25,000 km² in southern Colorado and Utah. The basin extends northwestward from the Four Corners area.

In the deepest part of the basin, the evaporite units have flowed extensively so that they now form a northwest-trending belt of salt-cored anticlinal structures (Cater, 1970). The Salt Valley anticline lies at the northwest end of this belt. Solution by ground water near the surface of these linear diapirs has resulted in the collapse of younger strata into long graben structures. In the Salt Valley anticline, the caprock of insoluble residue lies at the surface and extends downward for 200-250 m. Additional details on the geologic setting can be found in Hite and Lohman (1973) and Gard (1976).

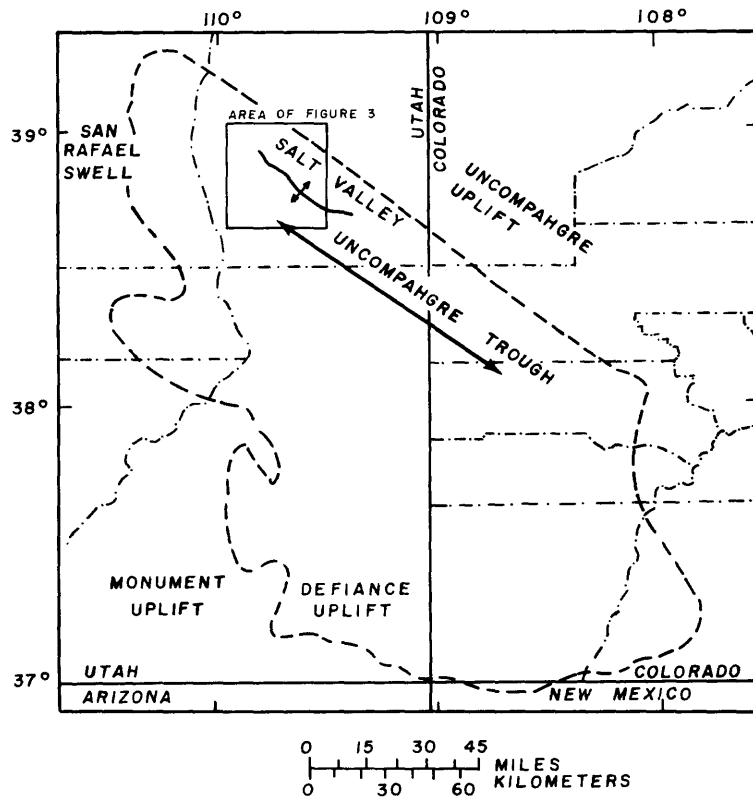


Figure 1.--Map showing the approximate limits of the Paradox Basin (---) and the outline of the Salt Valley anticline study area (—), Grand County, Utah. County outlines are unidentified. (Modified from Hite and Lohman, 1973.)

STRATIGRAPHIC FRAMEWORK AND ASSOCIATED ACOUSTIC PROPERTIES

The post-Mississippian lithologies in the salt-anticline region and their acoustic properties are summarized in table 1. The Paradox salt is the principal diapiric rock in the Paradox Basin. Original thickness of the salt may have been 1,500-2,500 m (LeFond, p. 21, 1969), but solution and plastic flow have completely eliminated the salt in some areas while concentrating as much as 4,300 m of halite in the adjacent anticlinal cores.

INVESTIGATIVE PROCEDURES

The investigation of the Salt Valley anticline region was divided into four phases:

1. Acquisition of seismic-reflection data and analysis of field parameters.
2. Processing of experimental seismic data in order to obtain maximum resolution from the existing seismic profiles.
3. Creation of synthetic seismograms from integrated acoustic logs and their correlation with the seismic data and other subsurface well-log information.
4. Computer modeling of hypothetical subsurface geology.

Seismic Field Parameters

Three multifold common-depth-point seismic profiles, one directly over the Salt Valley anticline, were obtained from the petroleum industry (fig. 2, profile line C). Because lines A and B (figs. 3, 4) are proprietary data, their locations are not shown on figure 2. The principal area of interest was the deeper flank and basal Mississippian sediments rather than the interior salt structure. A summary of the seismic field parameters for the three profiles is presented in table 2. The seismic sections for lines A, B, and C appear in figures 3, 4, and 5, respectively. Line C (fig. 5) is over the northwestern end of the Salt Valley anticline where the northwestward-plunging trend is interrupted by a small saddle and a structural knob (figs. 2, 6). The low-frequency, band-limited appearance of the seismic data is a result of a Vibroseis¹ source having a sweep of 45-6 Hz. The graben structures in the Mississippian acoustic basement at the base of the salt were the primary target. Lack of resolution of closely spaced events at these shallower depths is evident throughout the section; the edge of the salt diapir is poorly defined. The length of the geophone spread, as well as the distance to the near trace (>800 m) on line C, further suggests that an oil-exploration seismic profile is of limited value in the shallow resolution of intrasalt structure but will provide an excellent diagnostic tool in analyzing the growth history of the Salt Valley anticline as related to regional tectonics.

Sections A (fig. 3) and B (fig. 4) were recorded using dynamite as a source. The broad-band nature of this impulsive source is readily apparent, and mapping of very shallow (150-300 m), very thin (<50 m) reflector beds is possible. Shallow reflections on the flanks of the salt are clearly defined. A major disadvantage of the use of dynamite or other high-energy impulsive seismic sources is the inherent lack of control of the exact frequency and

¹Use of brand names in this report is for descriptive purposes only and does not constitute endorsement by the U.S. Geological Survey.

Table 1.--Paleozoic and Mesozoic stratigraphy and acoustic properties of the northwest Paradox basin
 [Modified from Hite and Lohman, 1973]

System	Stratigraphic unit	Thickness (meters)	Lithology	Acoustic properties		
				Velocity (m/s)	Density (g/cm ³)	
CRETACEOUS	Mancos Shale	±610	Dark-gray, fissile, marine shale	3,850-3,950	2.30-2.32	
	Dakota Sandstone	6- 60	Interbedded sandstone and conglomerate, carbonaceous shale, impure coal	3,725-3,825	2.36-2.41	
	Burro Canyon Formation	0- 90	Sandstone and conglomerate, green and reddish-purple shale			
	Brushy Basin Member	90- 230	Variegated, bentonitic mudstone, siltstone, red sandstone, conglomerate, limestone beds	3,275-3,400	2.29-2.35	
JURASSIC	Salt Wash Member	70- 135	Lenticular sandstones, few thin limestones	3,200-3,300	2.31-2.35	
	Summerville Formation	0- 30	Thin-bedded sandstone, sandy shale, and mudstone			
	Entrada Sandstone	Moab Member	0- 90	White, crossbedded, fine-grained sandstone	3,100-4,250	2.35-2.49
		Slick Rock Member		Crossbedded, buff, orange, and white, fine-grained sandstone		
		Dewey Bridge Member		Red, earthy sandstone and siltstone; contorted bedding		
	Navajo Sandstone	0- 150	Buff and gray, crossbedded, fine-grained sandstone	3,850-3,950	2.40-2.42	
	Kayenta Formation	0- 90	Lenticular, channel sandstone, siltstone, and mudstone	3,750-3,900	2.39-2.43	
		0- 150	Fine-grained, reddish-brown, thick-bedded, massive, and crossbedded, cliff-forming sandstone			
	TRIASSIC	Chinle Formation	0- 230	Reddish siltstone, sandstone, mudstone, and some conglomerate	4,150-4,300	2.45-2.55
		Moenkopi Formation	0- 335	Brown shale, mudstone, arkosic sandstone, and conglomerate. Thin beds of gypsum near base		
Cutler Formation		0-2,750	Red, arkosic sandstone and conglomerate. Some red sandy siltstone and mudstone	4,200-5,350	2.53-2.57	
PERMIAN	Rico Formation	0- 175	Similar to Cutler, but contains few beds of marine limestone	4,575-4,700	2.46-2.55	
	Upper member	0- 670	Fossiliferous, gray limestone, shale, and lenticular sandstone			
PENNSYLVANIAN	Paradox Member	0-4,280±	Salt, dolomite, gypsum, carbonaceous shale, and sandstone	±4,480	2.12-2.16	
	Molas Formation	0- 200				

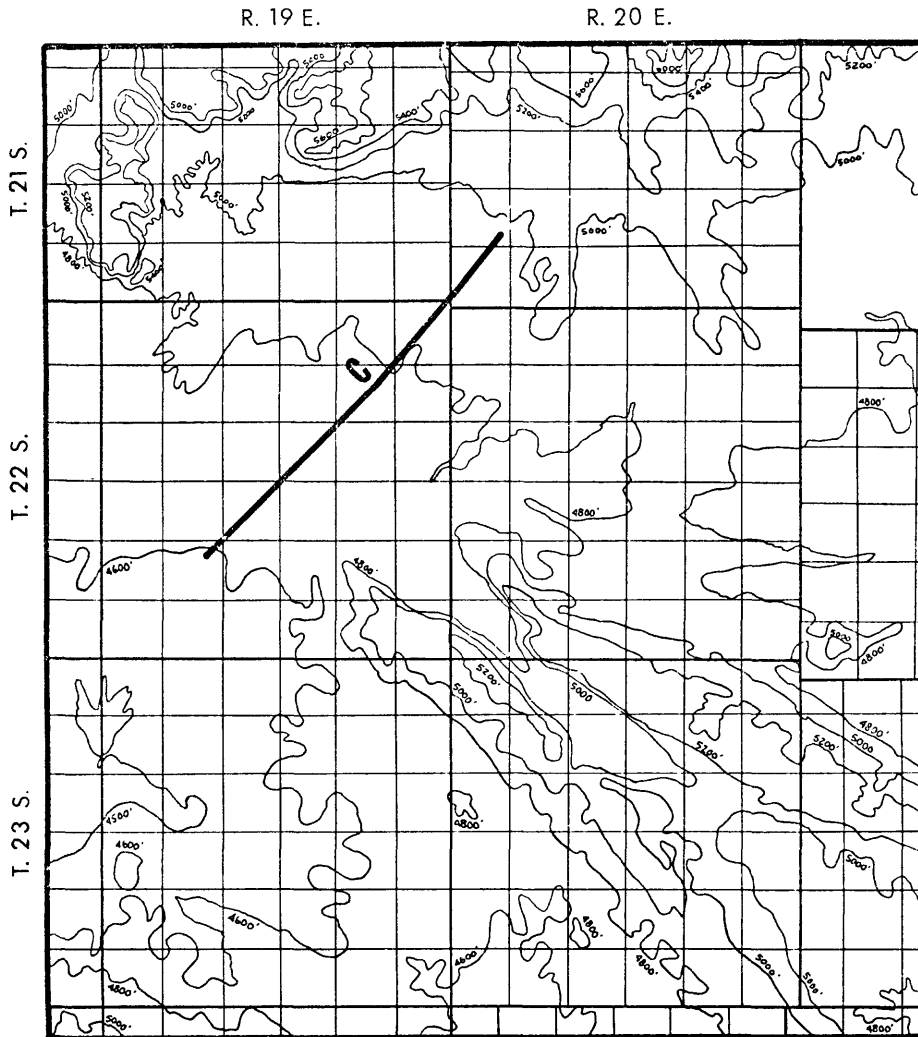


Figure 2.--Location of seismic profile line C over the Salt Valley anticline.

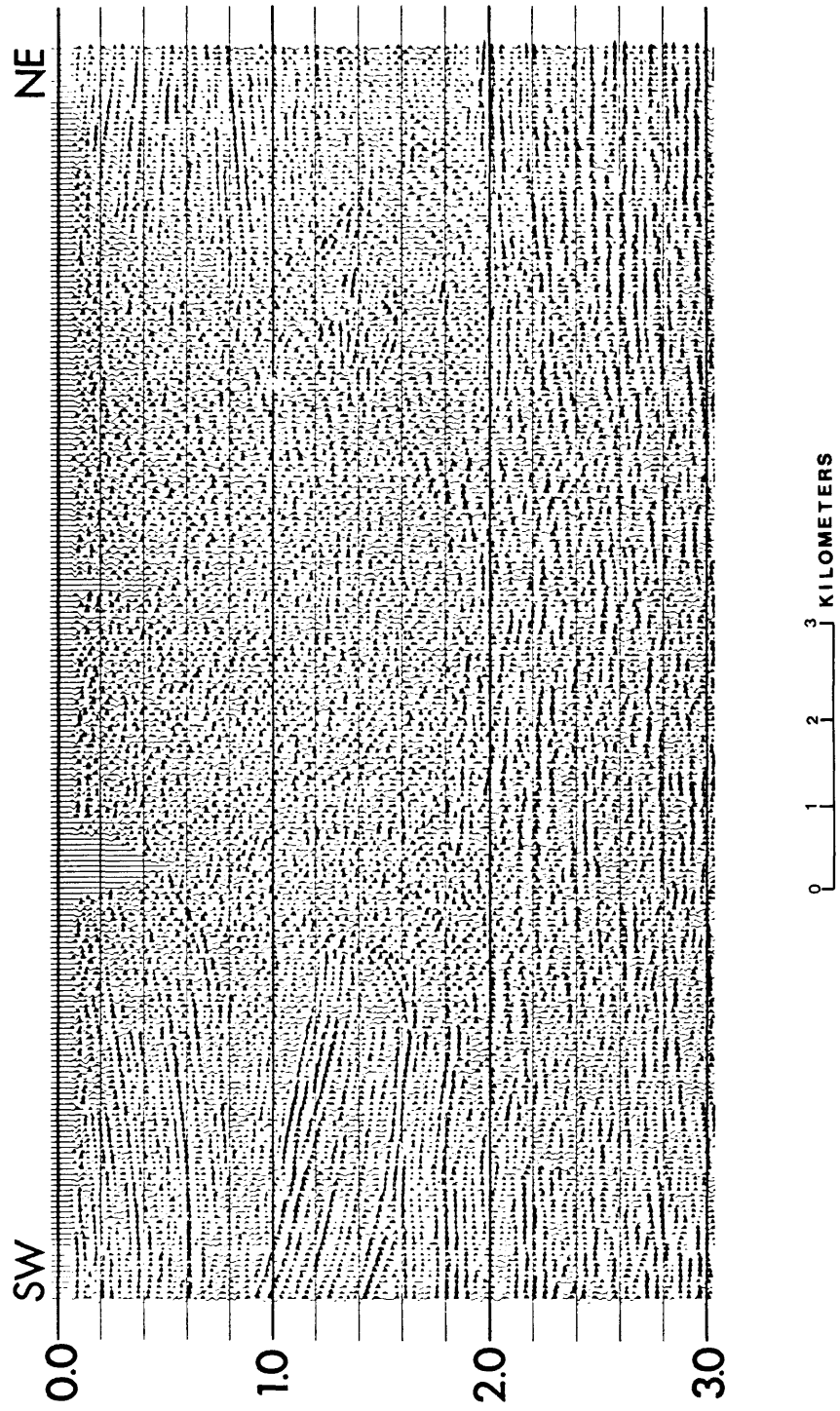


Figure 3.--Multifold, common-depth-point seismic section along profile line A.

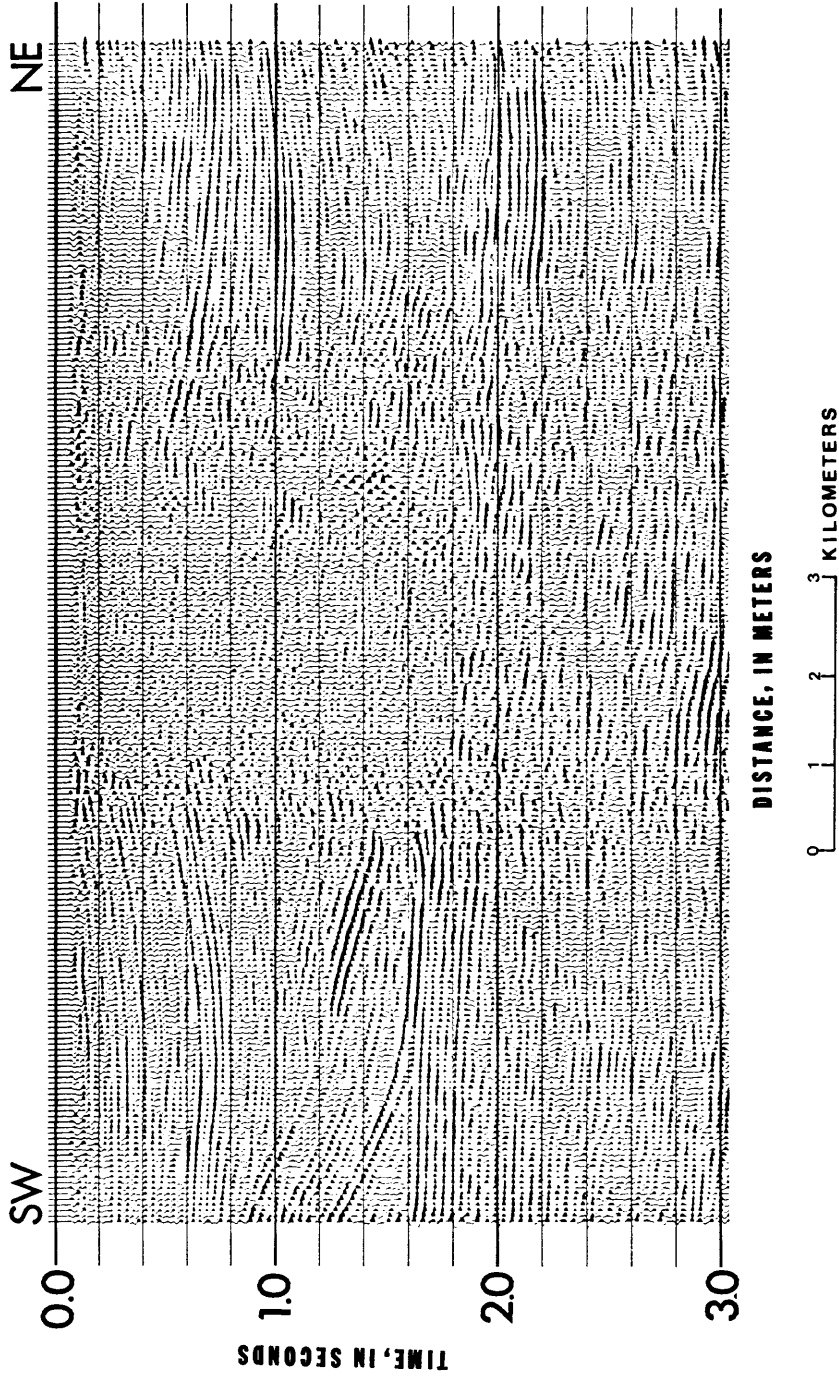


Figure 4.--Multifold, common-depth-point seismic section along profile line B.

Table 2.--Summary of seismic field parameters
 [Leaders (---) indicate no data available]

Field parameter	Line A	Line B	Line C
Energy source	Dynamite	Dynamite	Vibroseis
Pattern	3 holes	3 holes	3 holes
Geophones			
Pattern	Inline	Inline	Inline
Number per station	32	32	84
Group interval	450 ft	450 ft	440 ft
Spread	5400-450-0-450-5400	5400-450-0-450-5400	6600-2640-0-2640-6600
Instruments	Analog	Analog	Analog
Field filter	20-20-100 Hz	20-20-100 Hz	6-45 Hz
Record length	5.0 s	5.0 s	17 s
Sweep length	---	---	13 s
Type of gain	Automatic gain control	Automatic gain control	Automatic gain control
Fold	Twelvefold common depth point	Twelvefold common depth point	Twelvefold common depth point
Number of channels	24	24	20

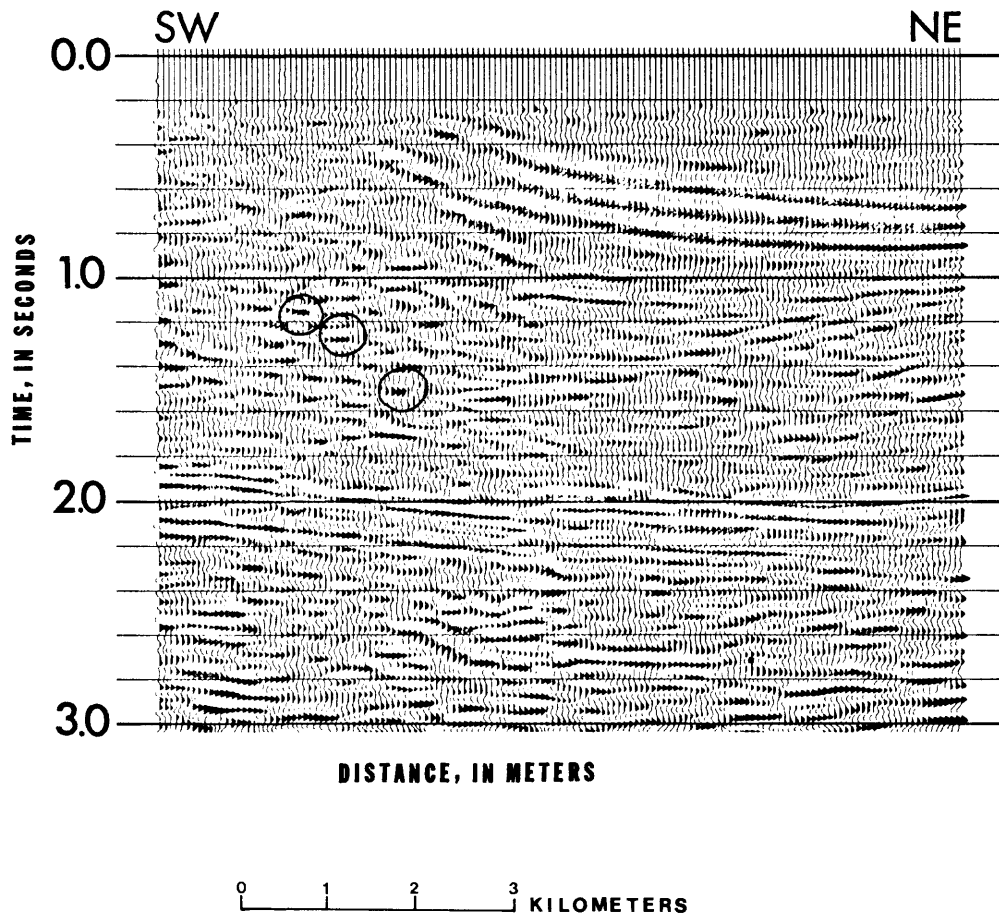


Figure 5.--Multifold, common-depth-point seismic section along profile line C. Areas circled are short-segment, en echelon seismic events.

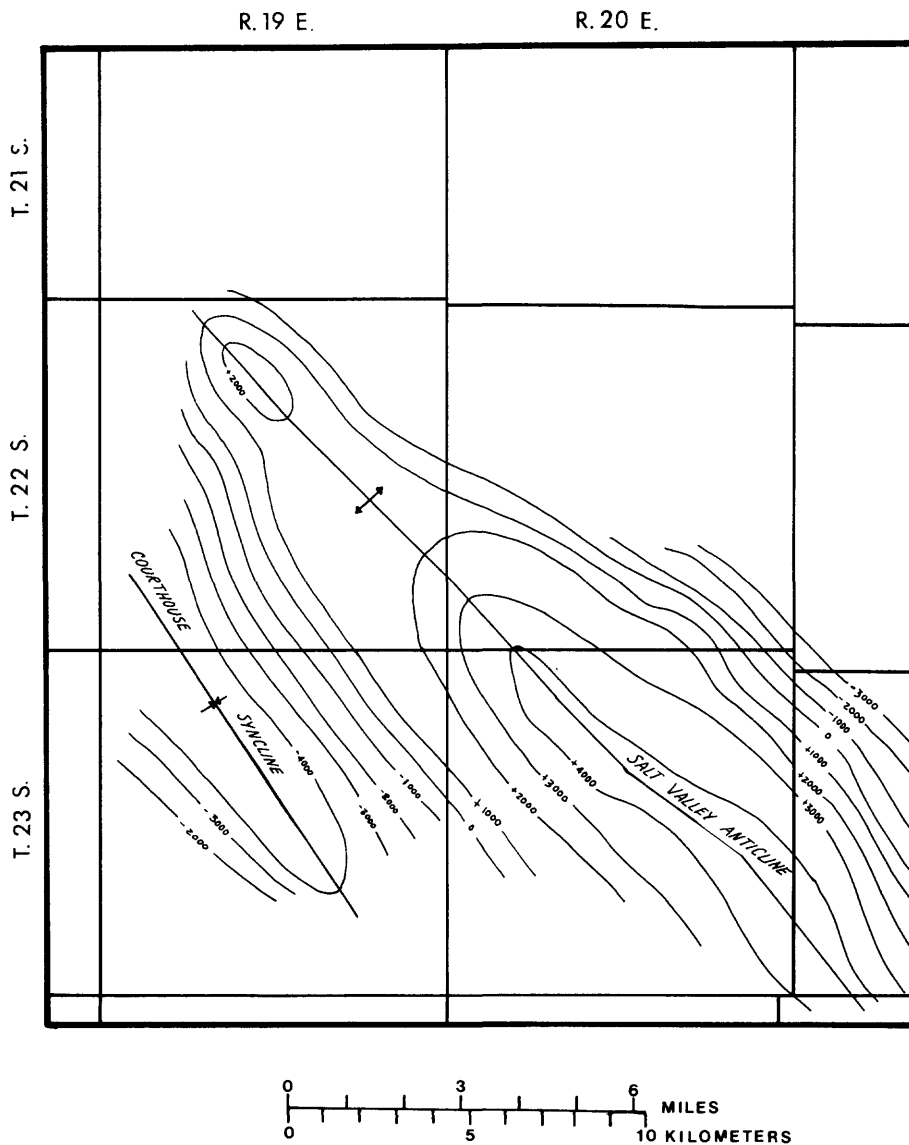


Figure 6.--Structure contours on top of salt of the Paradox Member of the Hermosa Formation in the Salt Valley anticline. (Modified from Hite and Lohman, 1973.)

phase character of the source determined by ground coupling, charge size, depth, and type of source.

Seismic Data Processing

Extensive analysis of the seismic data was performed in order to establish the processing parameters and sequence shown in figure 7.

Figure 8A shows an autocorrelation amplitude spectrum of a selected trace from line C. Several such analyses were used in determining the optimum deconvolution parameters and as a quality-control check on the effectiveness of the deconvolution in attenuating redundant information on the seismic traces. Severe 13-Hz ringing is evident on the seismic traces. A deconvolution-operator length of 0.140 seconds, which spanned roughly 1.5 cycles of the autocorrelogram, was selected. This operator was thought to be long enough to attenuate short-period redundancies on the data, but short enough to avoid attenuation of closely spaced primary events with similar spectral character. The results, as observed in the frequency analysis of figure 8B, show excellent spectral whitening and attenuation of the 13-Hz ringing. There are still some longer period redundancies, but common-depth-point stacking normally will effectively reduce their amplitude.

After deconvolution and bandpassing filtering, a velocity analysis was performed at close intervals along each profile in order to determine the optimum velocity to use in the computer-stacking routines. For nonparallel, dipping reflector beds, like those in the Salt Valley anticline, stacking velocity is related to, but not equal to, actual rock velocity.

Variations of thickness and velocity in the near surface can often introduce time shifts (static shifts) on the recorded trace. They can destroy the desired reflections when the data are stacked. With these data, as near-surface layer characteristics were not accurately known, a processing technique known as "automatic residual static corrections" was used to statistically derive the static time shifts in the data. After automatic static corrections, a tenfold stack was performed on line C; twelvefold stacks were performed on lines A and B.

The recorded time of a seismic reflection from a steeply dipping layer cannot be directly converted to depth because the time does not represent a vertical travel path. The processing techniques of migration (figs. 9, 10) correct for a nonvertical travel path. In order to enhance coherent, dipping events within a range of geologically possible dips, "a coherency filter" routine was applied to the data after migration.

An acoustic log obtained near the profile lines was used to estimate the velocities of the horizons in the stratigraphic column. A synthetic seismogram (fig. 11) was then created and compared to the processed seismic sections. As illustrated in figure 12, the synthetic section compares rather well with the processed section. This gives us a high level of confidence that the data have been processed correctly and that the various seismic horizons are properly identified.

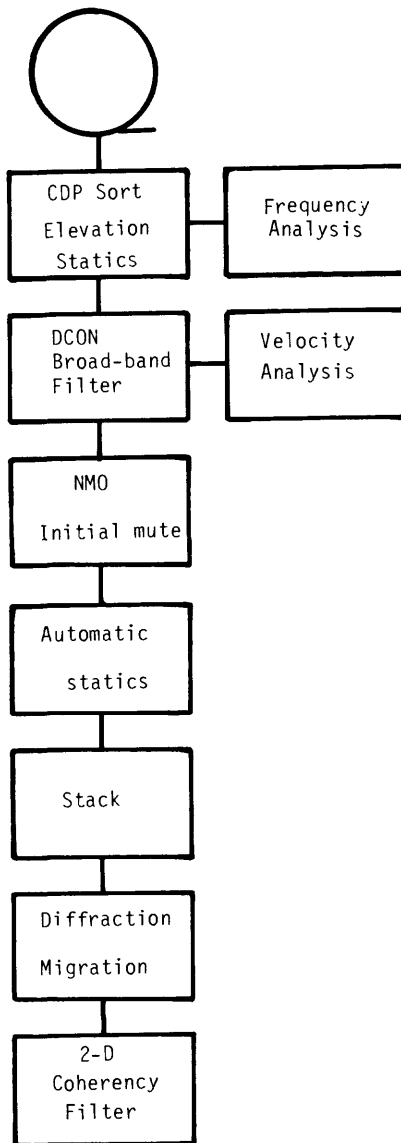


Figure 7.--Flow chart of the Paradox Basin data-processing sequence. CDP, common-depth-point; DCON, deconvolution; NMO, normal move out; 2-D, two-dimensional.

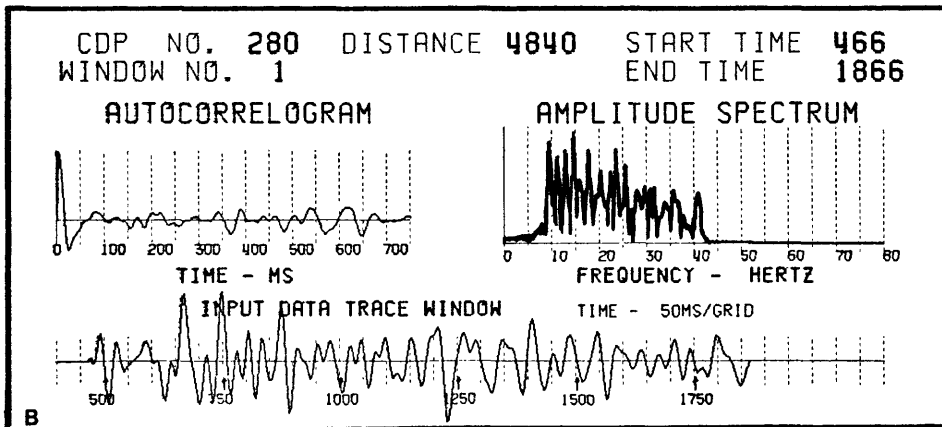
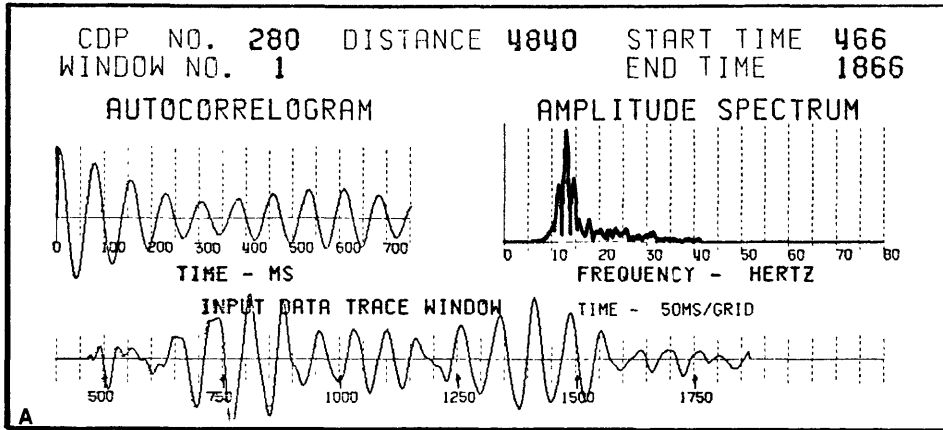


Figure 8.--Frequency analyses. A, before deconvolution of indicated interval and B, after deconvolution of indicated interval.

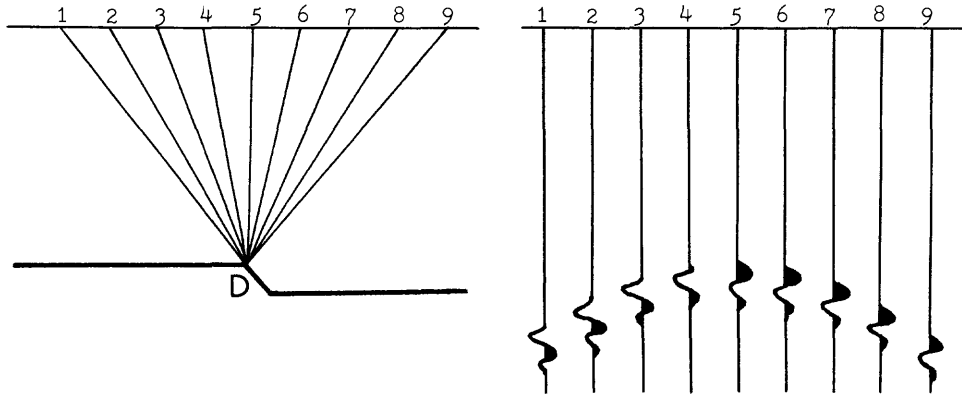


Figure 9.--Diffraction of seismic energy. A, depth section with sharp acoustic contrast at D, diffracting seismic energy in all directions and B, corresponding seismic time profile.

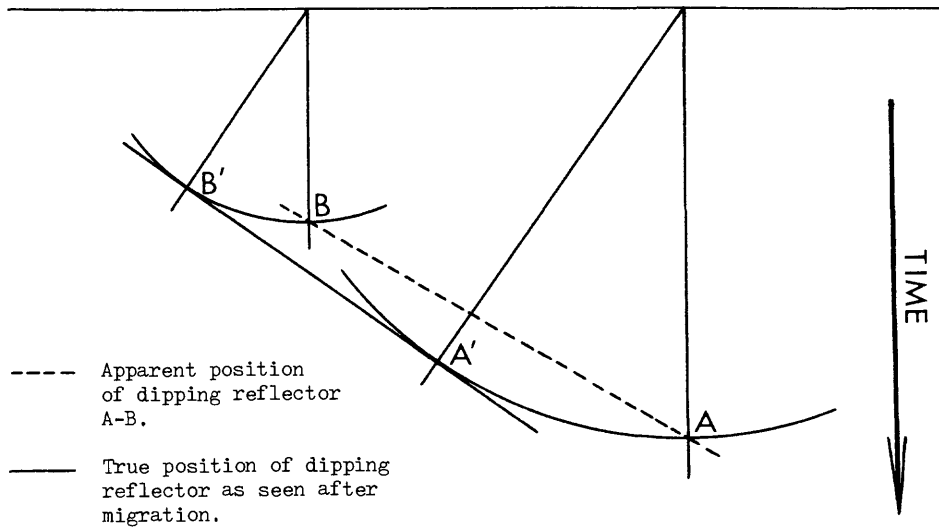


Figure 10.--Migration of seismic events due to dipping beds.

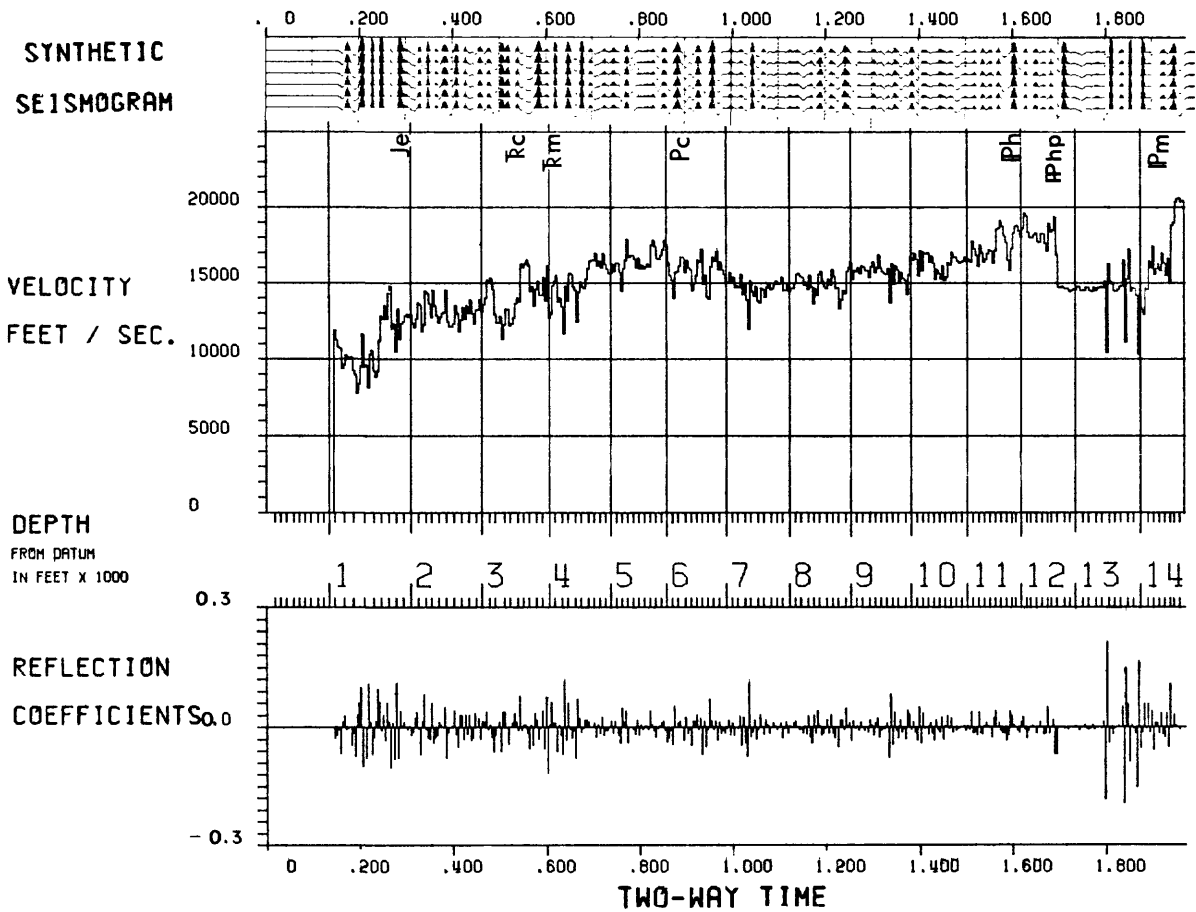


Figure 11.--Synthetic seismogram from an acoustic log. Pm, Molas Formation; Php, Paradox Member of Hermosa Formation; Ph, Hermosa Formation; Pc, Cutler Formation; Rm, Moenkopi Formation; Je, Entrada Formation.

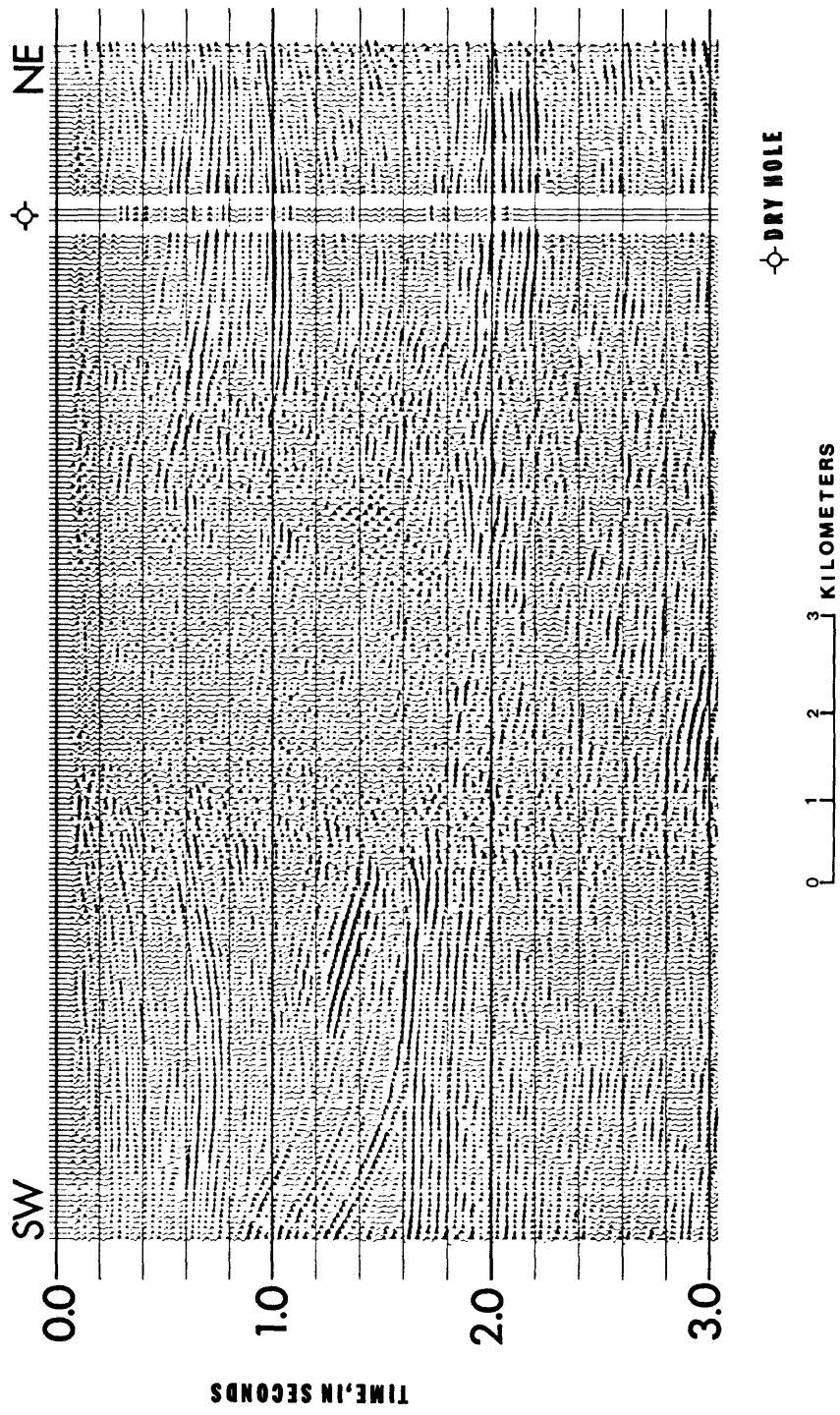


Figure 12.--Section B with synthetic seismogram from figure 11.

INTERPRETATION OF SEISMIC DATA

Figure 12 shows the approximate correlation between the acoustic log synthetic and the seismic-reflection data. This correlation provided the basis for identification of the various reflectors on the seismic sections. This correlation, in turn, allows the interpretation of the growth history of the structure, including an analysis of the tectonic control of sedimentation and the relationship between the salt diapir and the adjacent structure. Further analysis of the data yields possible characterization of the intrasalt structure. Interpreted sections are presented in figures 13-15.

Structural Framework

The average seismic velocities in sediments adjacent to the Salt Valley anticline are close to that of pure salt. Owing to velocity differentials, little distortion of the Mississippian base-of-salt can be expected on the seismic time sections. The presence of a deep horst-graben system under the salt (fig. 15) lends credence to the concept of structural influence on, if not initiation of, the diapirism. However, the dramatic thickening of flank sediments toward the synclinal axes on either side of the salt ridge indicates positive sedimentary control of the upward movement of the halite. The data from profile line B (fig. 14) show roughly 1.6 s of seismic two-way traveltime from the top of the salt, which is near the surface, to the base of the salt. This time difference indicates that more than 3,500 m of salt is at the anticlinal axis. This thickness implies approximately the same amount of differential thickness in the adjacent sediments. The thinning toward the anticline of the upper member of the Hermosa Formation, as indicated on lines A and B (figs. 13, 14), suggests that diapirism had already begun by Middle to Late Pennsylvanian time. Initial salt diapirism was structurally influenced; but continued rapid sedimentation, associated with the removal of salt by flow from the flanks of the salt swell, maintained the upward momentum of the salt mass.

Some continuous seismic events appear within the salt on the processed sections. Several short isotime lineups of seismic events are apparent in a general en echelon pattern in the salt. There are no continuous indications of the presence of a reflector bed in the shallow salt; however, if the folding is of the suspected degree of complexity, these reflector beds could be connected by vertical segments (giving no reflections) or they could be transposition folds. A similar intrasalt reflection character is evidence on lines A and B, although noise obscures these reflections. Another possible origin of these coherent seismic events, which will be discussed in more detail in the modeling section of this report, is that the segments represent buried foci due to concave-upward folding of the high acoustic contrast interbeds. In any case, these phenomena of the seismic sections are, at best, indirect. The exact shape and location of the interbeds is only implied. Because the absence of interbeds, rather than their presence, is of paramount importance in searching for a nuclear waste emplacement site, these phenomena alone may provide sufficient evidence to suggest the presence of an interbed. High-resolution seismic profiles could provide a more direct indication of the nature of the interbeds. Closer spacing of seismic surface

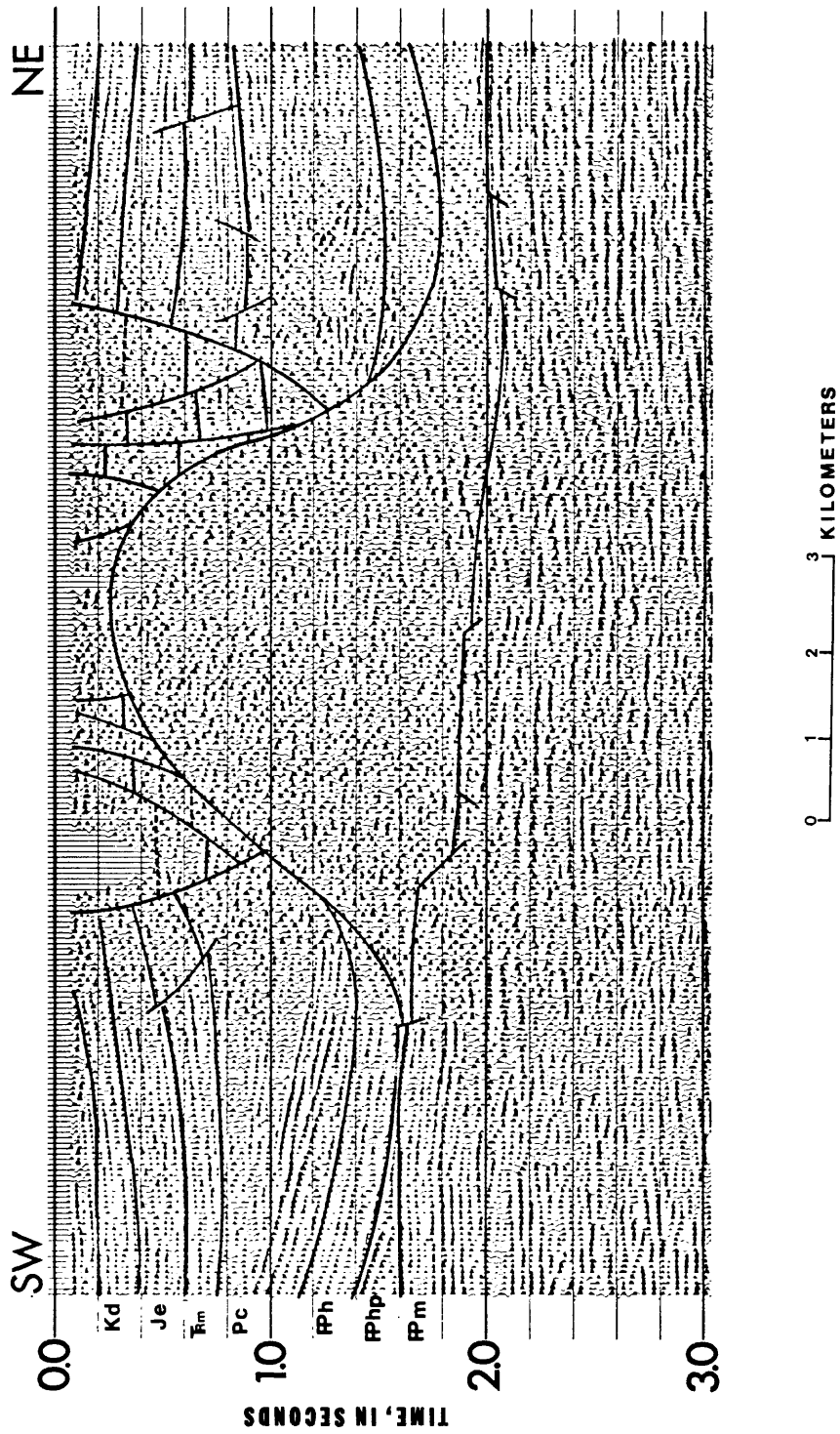


Figure 13. --Section A (interpreted). Lines show configuration of faults and salt-anticline units on flanks. Pm, Molas Formation; Pph, Paradox Member of Hermosa Formation; Pph, Hermosa Formation; Pc, Cutler Formation; Rm, Moenkopi Formation; Je, Entrada Formation; Kd, Dakota Sandstone.

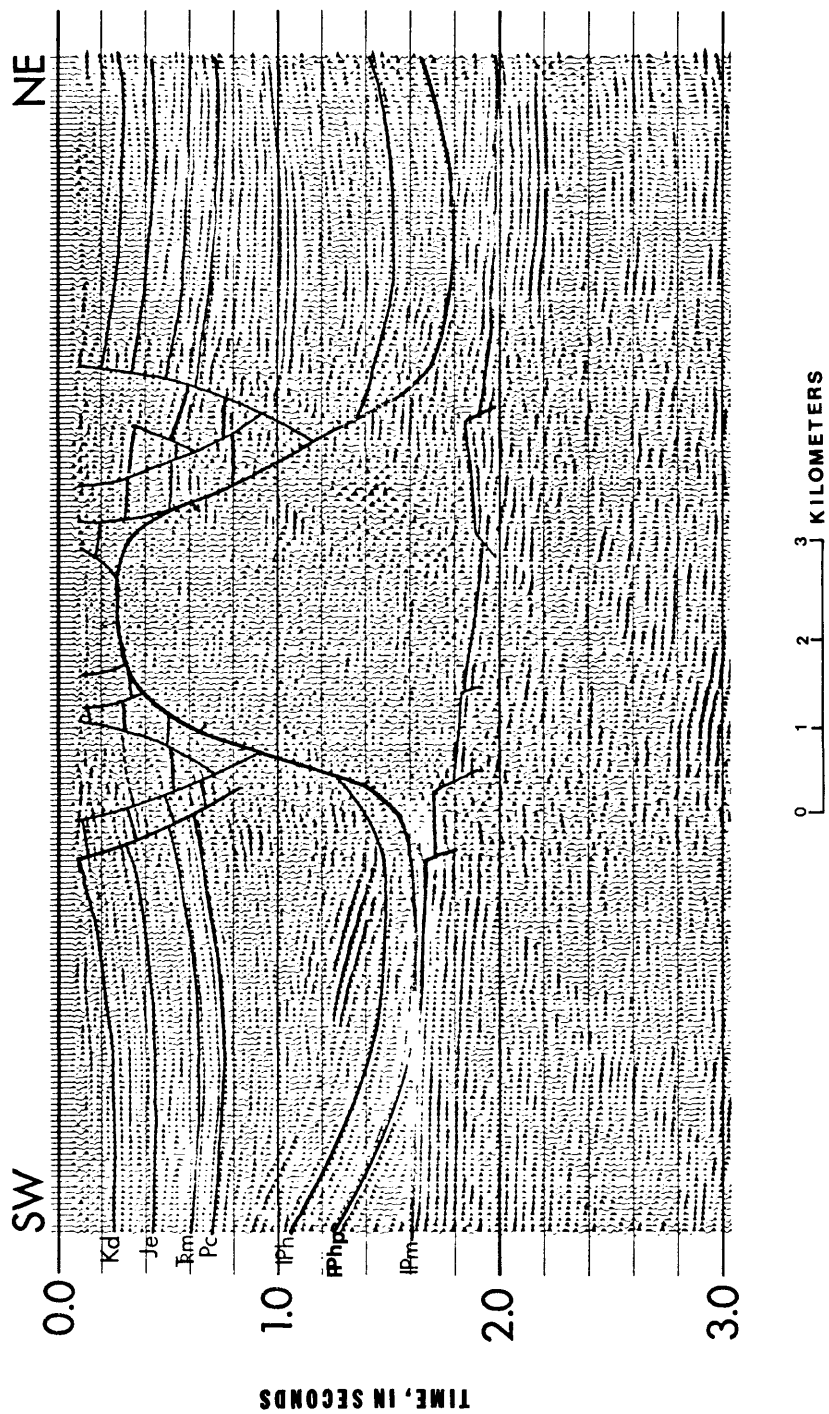


Figure 14.--Section B (interpreted). Lines show configuration of faults and salt-anticline units on flanks. IPm, Molas Formation; IPhp, Paradox Member of Hermosa Formation; IPh, Hermosa Formation; Pc, Cutler Formation; T m, Moenkopi Formation; Je, Entrada Formation; Kd, Dakota Formation.

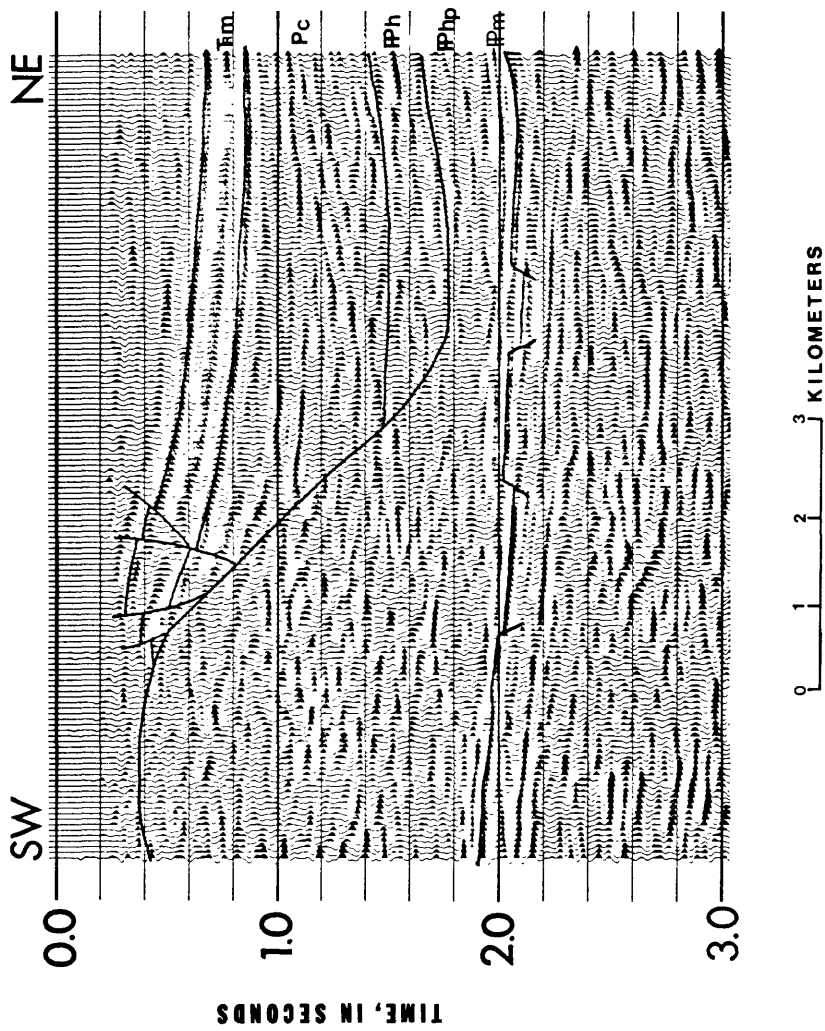


Figure 15.--Section C (interpreted). Lines show configuration of faults and salt-anticline units on flanks. Pm, Molas Formation; Php, Paradox Member of Hermosa Formation; Ph, Hermosa Formation; Pc, Cutler Formation; Pm, Moenkopi Formation.

stations would allow better coverage of complex folding in the subsurface, and higher frequencies should permit finer resolution. Computer subsurface seismic modeling was used as a consistency check on the geologic interpretation and as a determinant in designing a new seismic survey to locate the marker beds.

COMPUTER SUBSURFACE MODELING

Figure 16 shows our thin-beds model and figure 17 shows the resulting synthetic model. The top two wedges of low- and high-velocity material vary, respectively, from 0 to 150 m in thickness, and the wavelet closely approximates the impulsive source signature of sections A and B. It can be seen that constructive reinforcement of the wavelet from the salt-interbed boundary with that from the interbed-salt boundary obscures the true nature of the reflectors.

The distortion of the interbeds in the salt may provide a promising indirect indication of their presence. Figure 18 shows a hypothetical model of a severely folded thin bed imbedded in a saltlike medium. Buried focusing of the reflected energy, due to the presence of thin beds at depth, results in the seismic signature shown in figure 19. This indication of folded interbeds has the advantage of being relatively independent of the thickness of the interbed. This is an indirect, rather than a direct, method of detecting the presence of interbeds in the salt; and it depends on the geometry and degree of closure of the folds. If the shape of the interbed distortion conforms to the assumptions of Hite and Lohman (1973), this technique for mapping the interbeds is feasible.

Figure 20 shows a typical salt-ridge subsurface model derived from a composite of the three seismic profiles, the borehole information, and assumptions on the nature of the shallow faulting. Figure 21 shows the normally incident rays generated for the subsurface model of figure 20. The refraction of the rays at each interface has the effect of scattering the reflected energy from a small portion of the subsurface over a large portion of the time section. The many oblique ray paths indicate that many seismic events shown vertically beneath a source point will represent reflections from a considerable distance off the vertical.

The hypothetical cross section of the Paradox Valley anticline (Hite and Lohman, 1973) was modeled using three asymmetrically folded thin beds within the salt (fig. 22). Second-order folding, laterally varying velocity and density, were superimposed on these thin beds. Structural complexity of the interbeds increased toward the anticlinal core in the manner described by Kupfer (1968). The resultant synthetic seismic section is shown in figure 23. Figure 24 shows a synthetic section produced from the reflections from the interbeds only. Energy dispersion and diffraction are evident throughout the section. Many of the folds were tighter than the 100-m trace interval used in the model, making identification of the buried foci impossible. Diffraction migration of these data would aid the detection of the interbeds, but would require a high degree of precision in the determination of the migration velocities. The diffraction migration of the synthetic data would collapse the diffractions from the tight interbed folding and yield an intrasalt en echelon pattern similar to that observed on the real seismic data. (Compare circled areas on figs. 4, 24.)

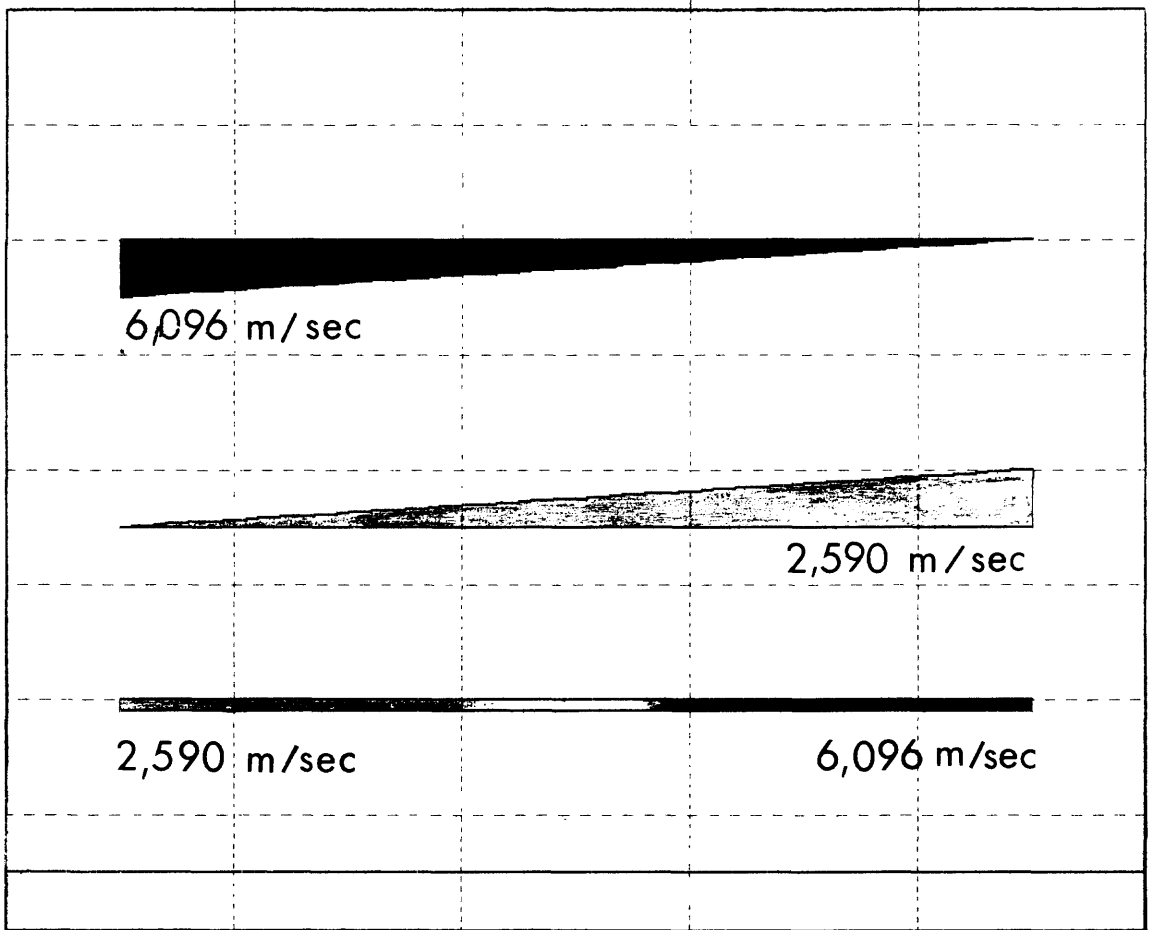


Figure 16.--Models of thin beds within salt showing thickness and velocity variations.
The velocity of the salt is 4,480 m/s.

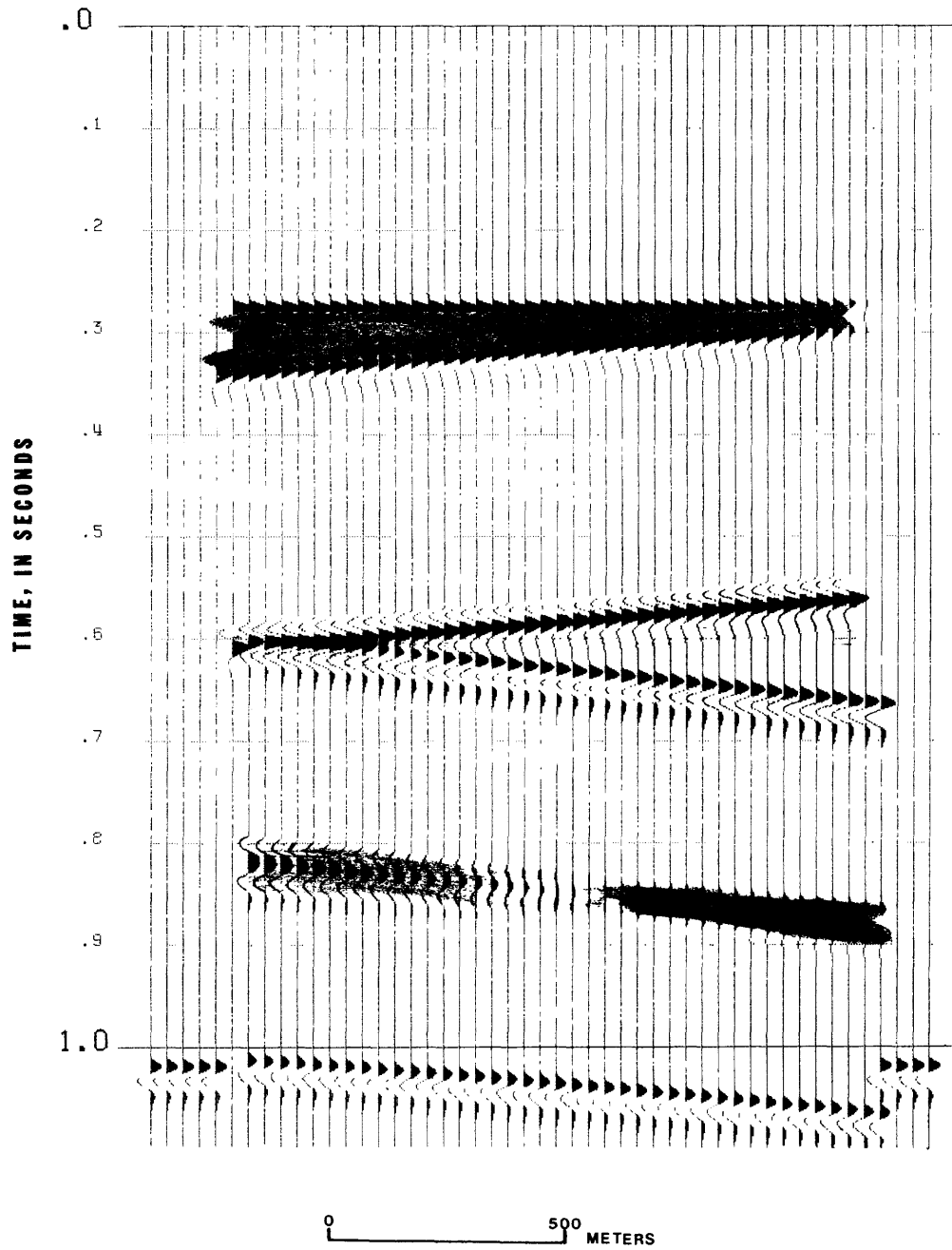


Figure 17.--Synthetic seismic sections of thin beds.

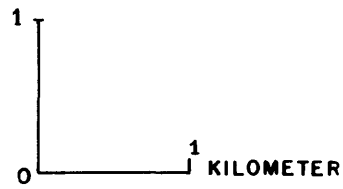
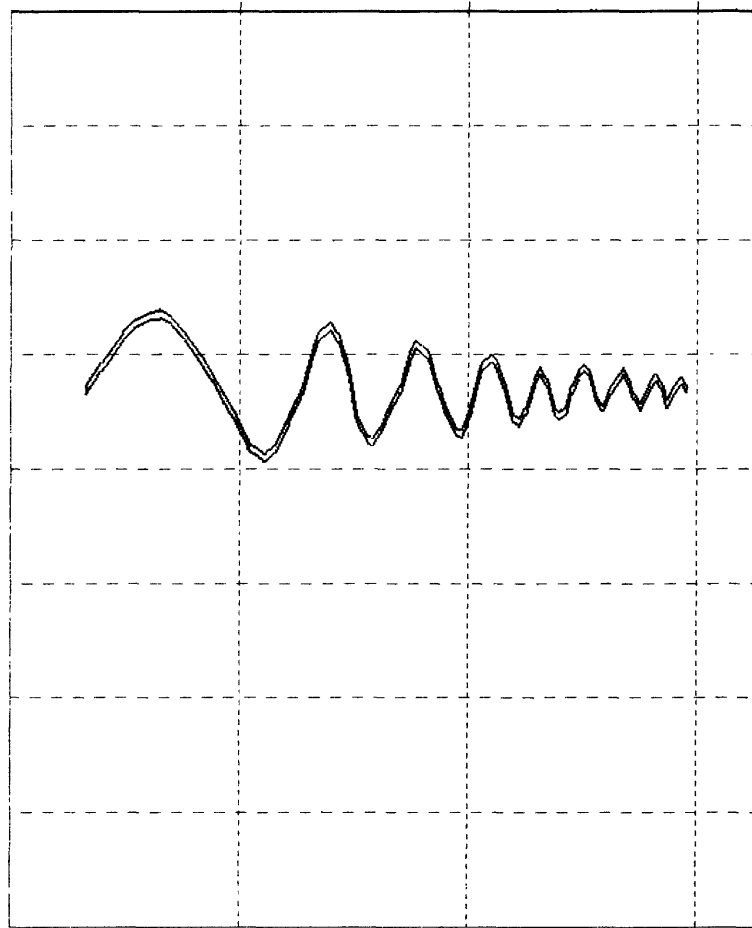


Figure 18.--Model of interbed in salt to observe the effect of the folding of thin beds in the seismic section.

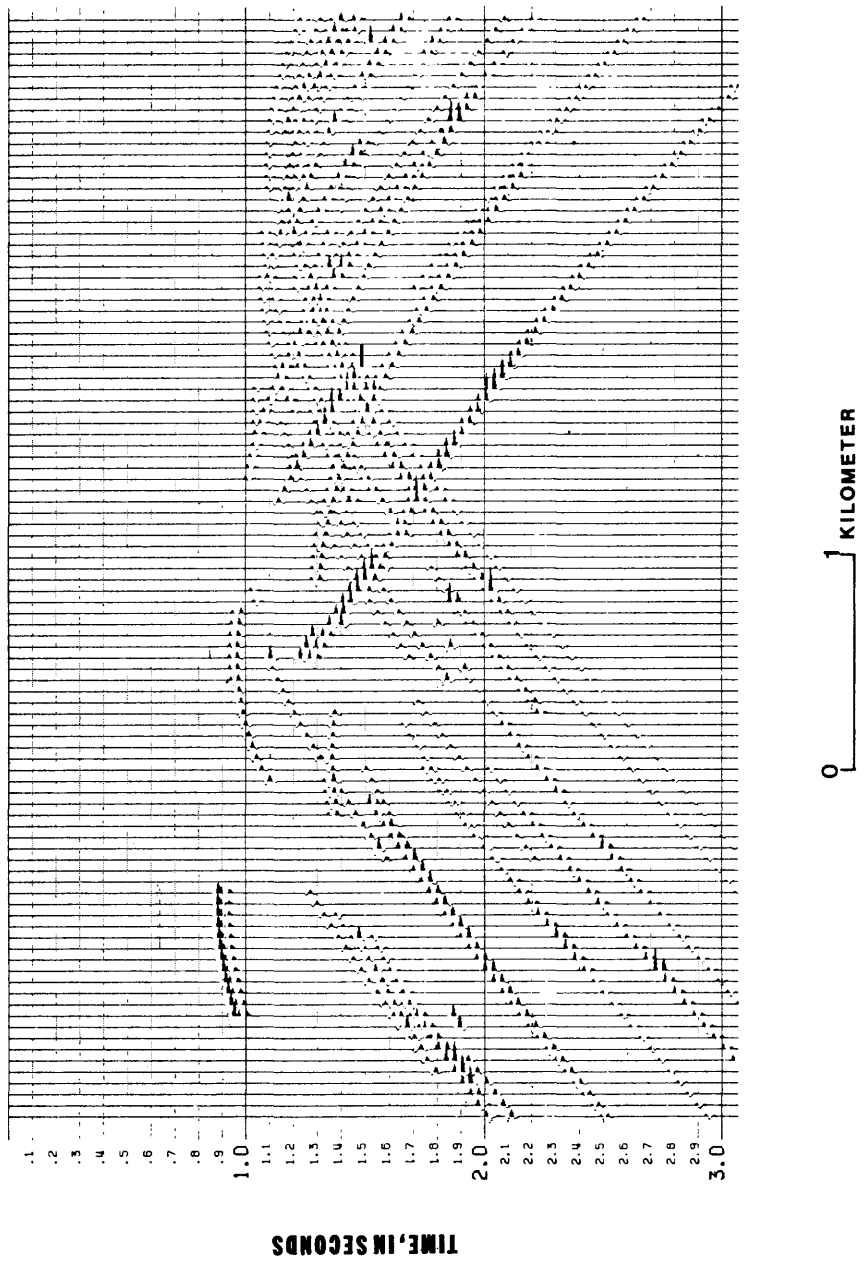


Figure 19.--Depth to seismic foci in buried and folded salt interbeds.

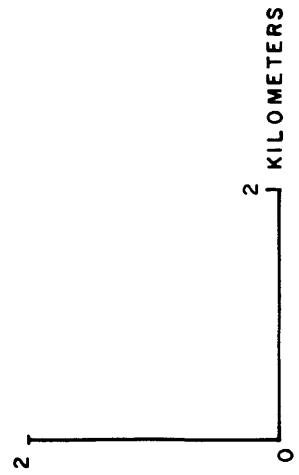
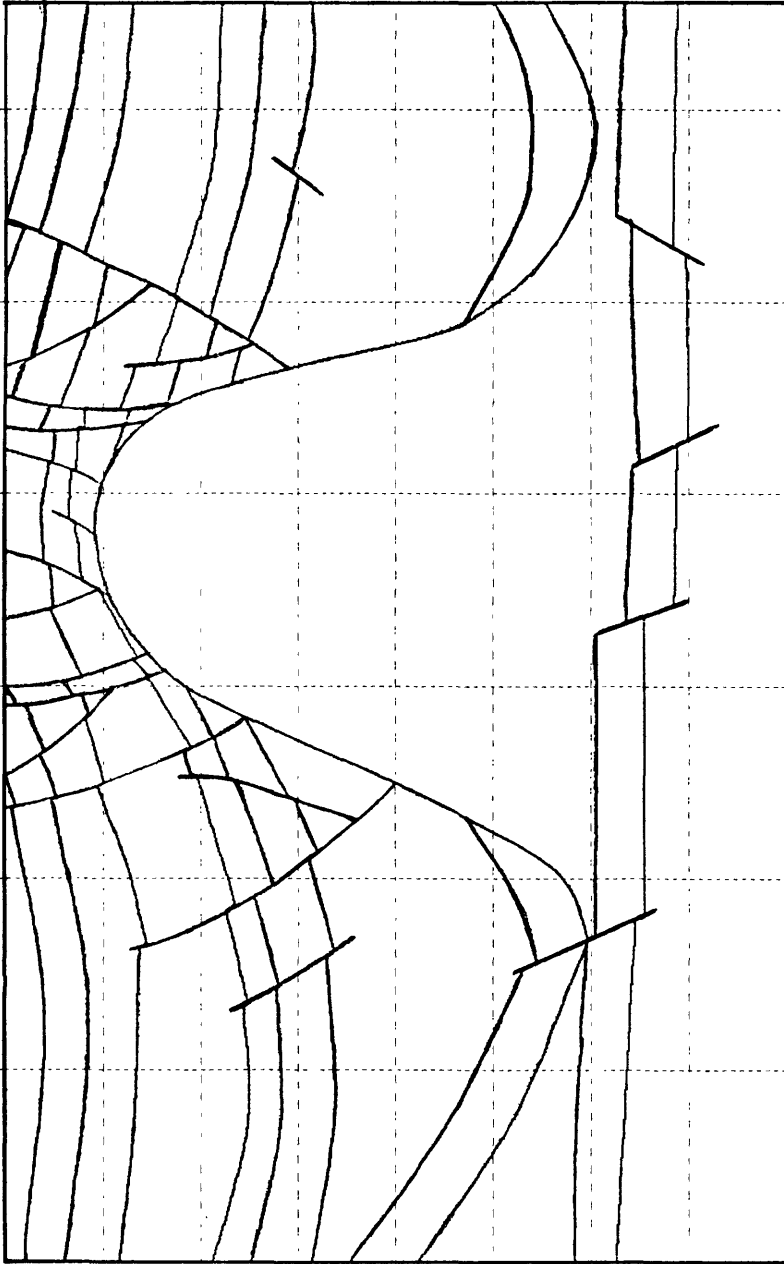


Figure 20.--Model of a typical subsurface salt ridge derived from a composite of three seismic profiles, borehole information, and hypothesis about the nature of the shallow faulting.

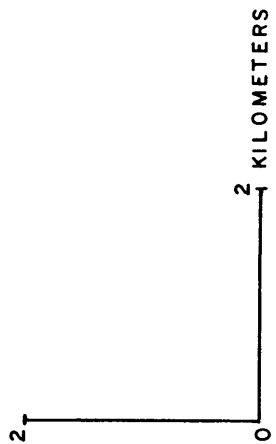
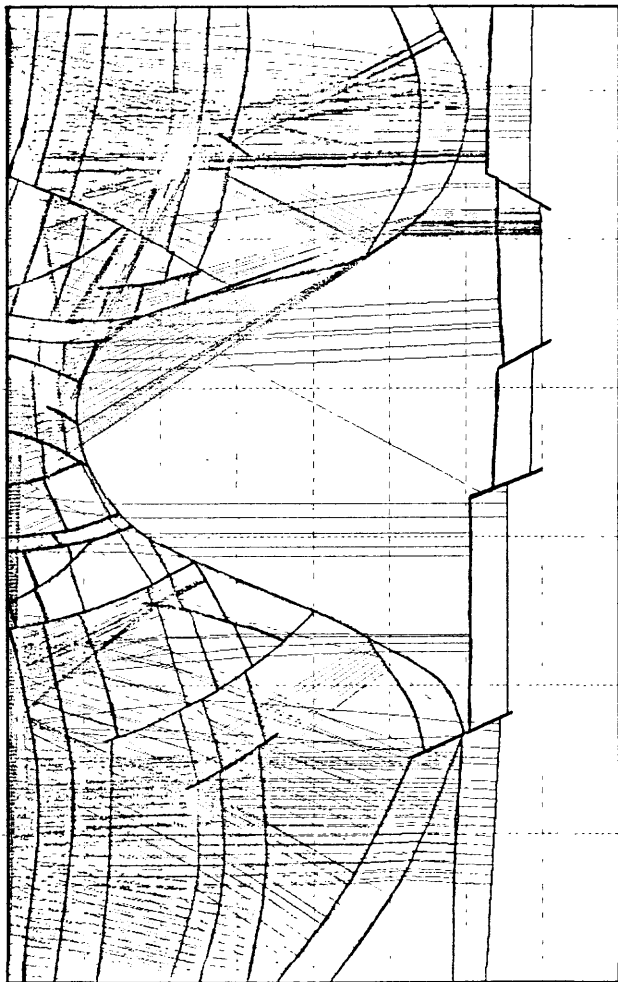


Figure 21.--Normally incident ray paths generated for the subsurface model of figure 20.

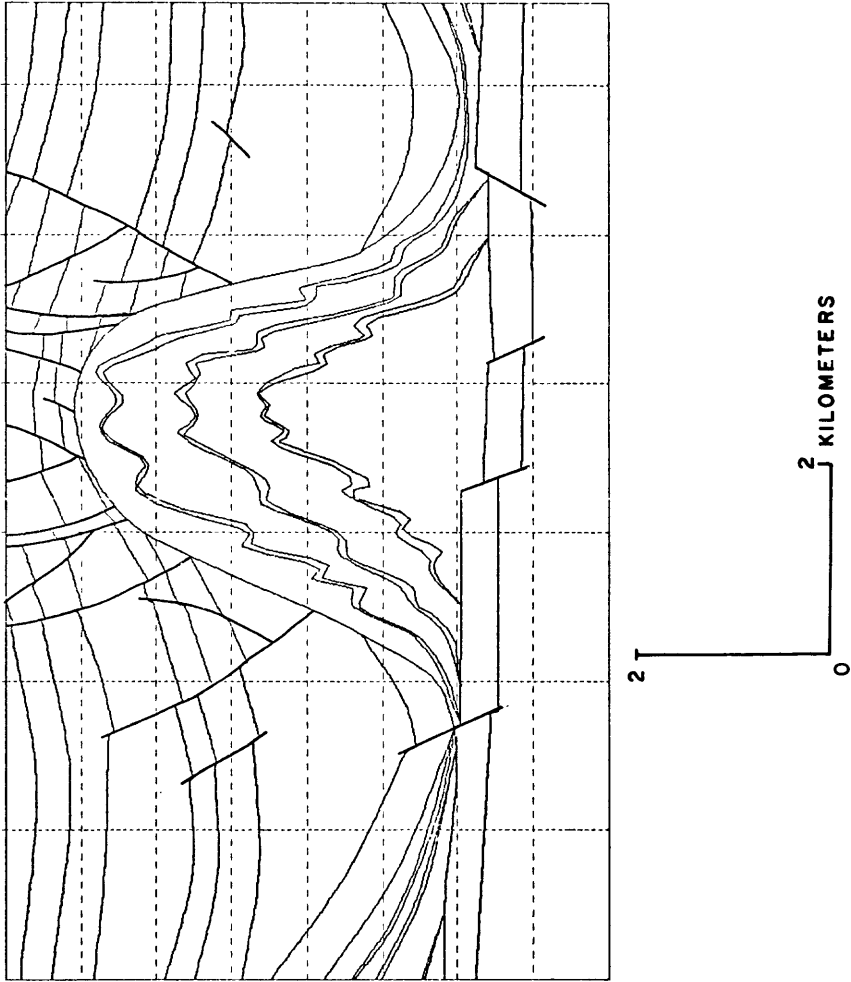


Figure 22.--Salt ridge and asymetrically folded interbeds.
(Modified from Hite and Lohman, 1973.)

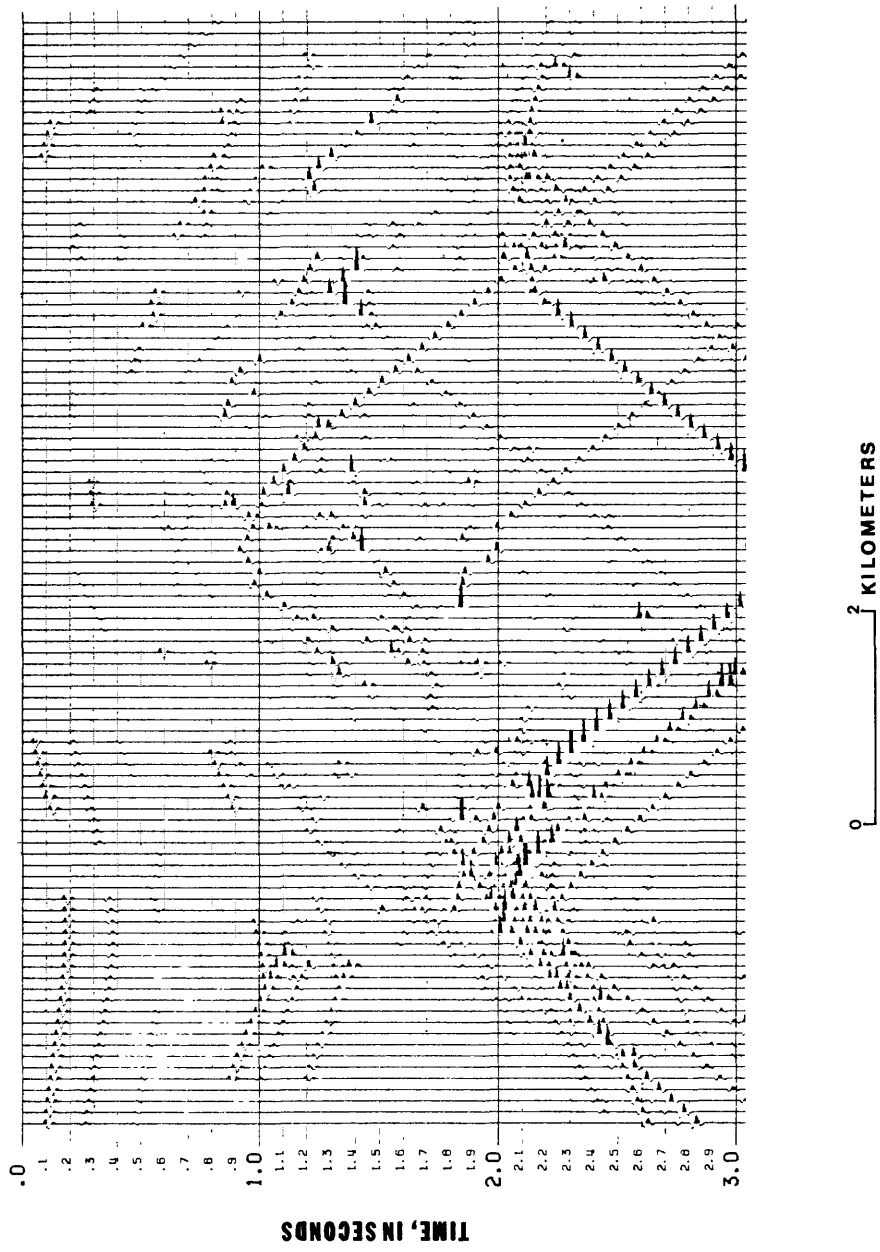


Figure 23.--Synthetic seismic record section showing salt interbeds.

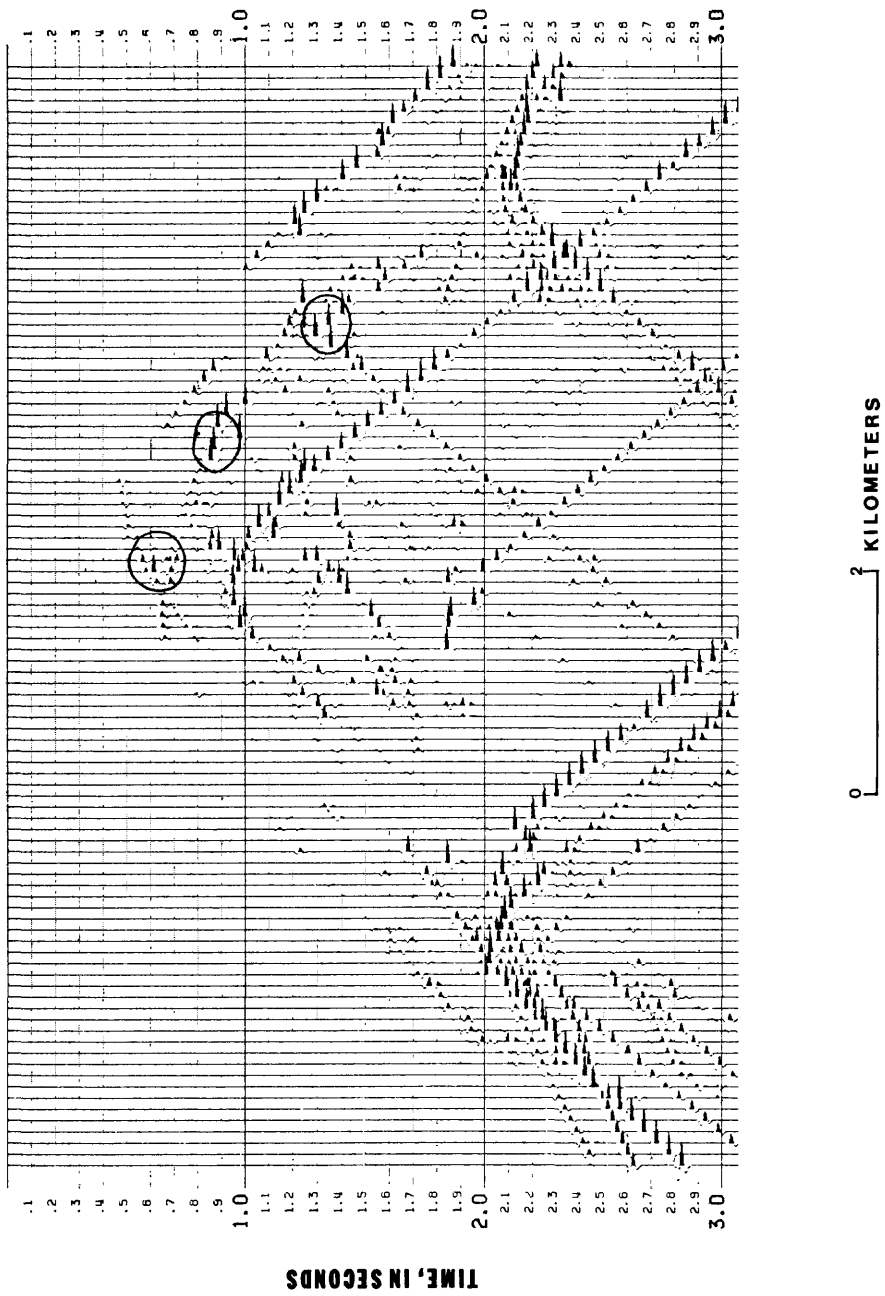


Figure 24.--Synthetic salt-ridge seismic record section produced from the interbed reflections only. Areas circled have similarities to observed seismic events on real data (fig. 5).

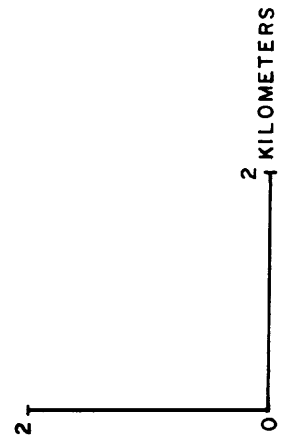
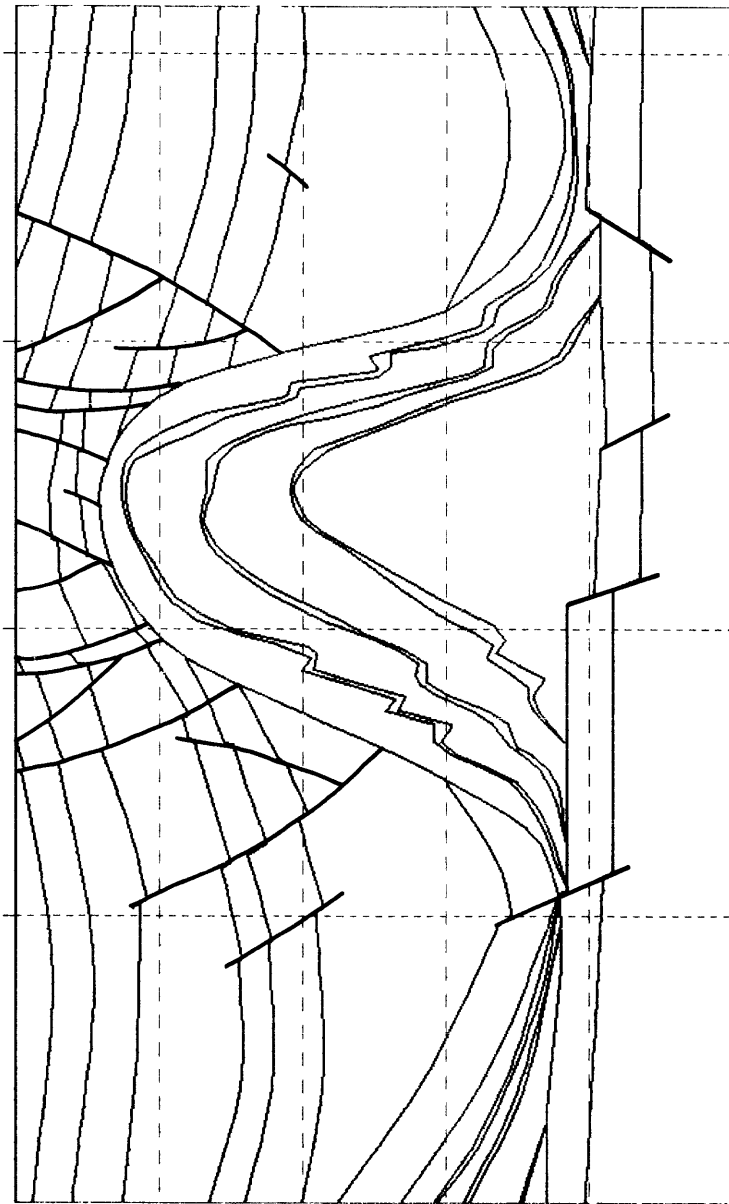


Figure 25.--Salt-ridge model with less complexly folded interbeds.

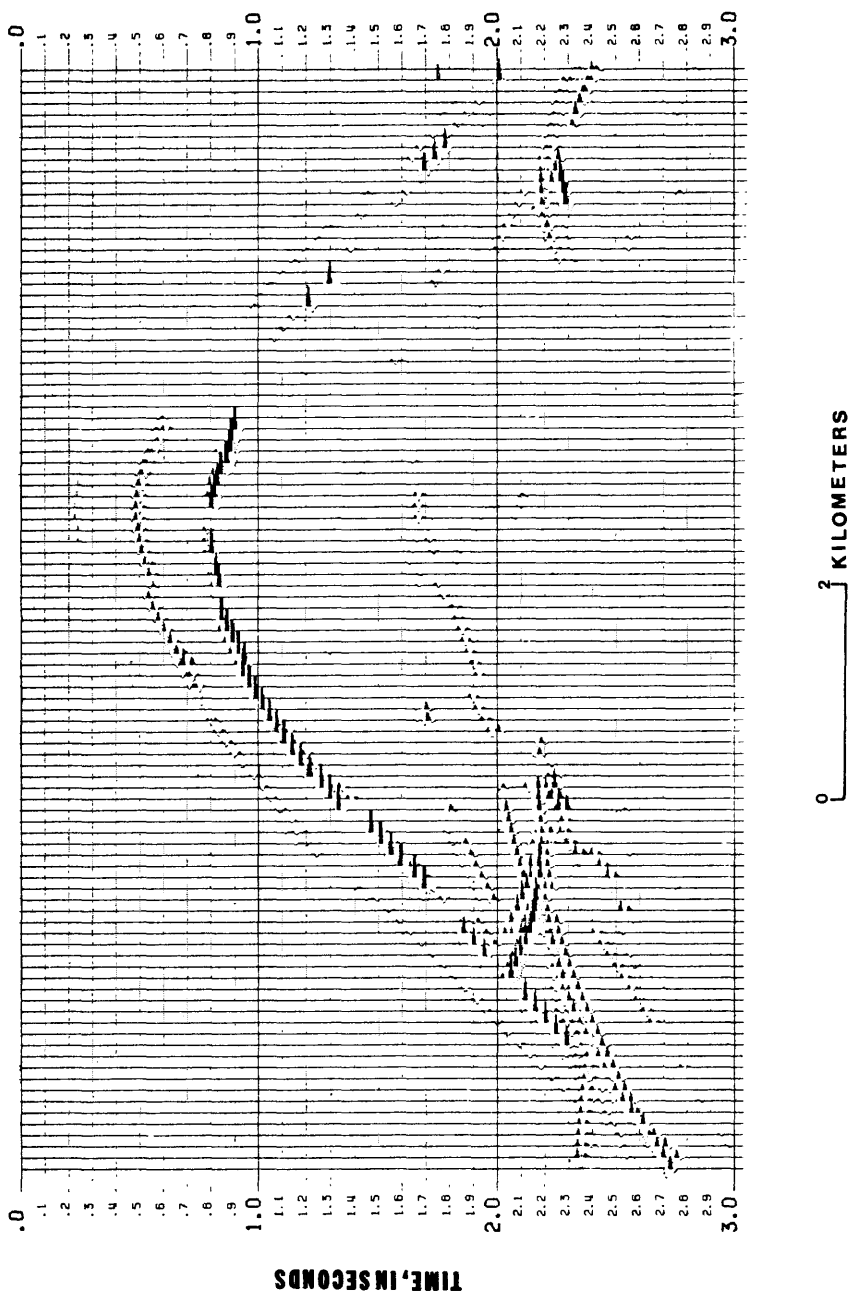


Figure 26.--Less complex synthetic seismic record section showing interbed reflections only.

The second salt-ridge model has a subsurface flank identical to that of the model shown in figure 20 but has less severe folding of the interbeds near the anticlinal axis (fig. 25). This type of folding would be expected if the principal stress axis were vertical rather than horizontal. The synthetic section, again showing only reflected energy from the interbeds, is presented in figure 26. Although the seismic response shows a proportional reduction in complexity, diffracted energy still dominates the seismic section. If, however, the shallower interbeds are less complex, mapping may be possible using conventional or nearly conventional seismic-reflection techniques.

RECOMMENDATIONS

Mapping of shallow, structurally complex reflector beds in an area such as the Salt Valley anticline requires a custom-designed, integrated geophysical program that will incorporate state-of-the-art techniques, such as vertical seismic profiling; shallow reflection surveys, possibly using a source with a known signature; and a detailed borehole survey. Potential field methods, such as gravity and magnetic anomaly mapping, would have limited usefulness owing to the suspected broad areal extent of the interbeds and the complexity of the rocks near the surface. Recent advances in seismic data processing can yield highly quantitative analyses of the subsurface and provide greatly expanded resolution of subtle acoustic differences in the geologic profile.

Vertical Seismic Profiling

Until recently, very little has been published on the use of vertical seismic arrays in the detailing of shallow acoustic boundaries. Studies by Gal'perin (1974), Wuenschel (1976), and others have only recently begun to exploit the advantages of VSP (vertical seismic profiling) as an exploration tool. Some of the advantages of VSP are as follows:

1. Improved signal-to-noise ratio. Placing either the source or the receiver arrays or both in a borehole below the inhomogeneous near-surface reduces wave scattering often encountered when using surface or near-surface arrays.
2. Broader bandwidth is obtainable owing to better rock coupling of both the source and the receiver. Expansion of the frequency bandwidth results in higher resolution, allowing the separation of closely spaced or thin reflectors on a seismic time section.
3. Directional sensitivity of three-component geophones in vertical seismic profiling would make possible three-dimensional analysis of the seismic response. Direction of the reflector from the receiver, dip information, and the determination of reflector characteristics from amplitudes and modes of wave propagation could be obtained.

Surface Seismic Methods

Because the principal depth of interest for nuclear waste emplacement is shallow (less than 1,200 m), the surface configuration of the seismic spread should have a short offset and a small interval between geophones. When the angle of incidence of the seismic wave with the reflectors is nearly normal, the effects of refraction and mode conversion of the seismic

energy are minimized. If the reflected seismic wave is approximately planar when it reaches the detectors, separation of the reflected energy from noise traveling horizontally (along the surface of the ground) is simplified. A spread length on the order of 350 m or less would insure that the angle of incidence would be quite high for a flat reflector. The short offset would further insure that the Rayleigh and Love waves generated by the source would not interfere with shallow, reflected energy. The depths of interest on a shallow seismic profile would be represented in less than 0.600 s of two-way time on the seismic section.

Small-interval short-spacing of geophones would have two advantages:

1. A closer reflection-point spacing on the subsurface profile would be equal to one-half on the geophone spacing. This would allow detection of smaller anomalies.
2. More geophones would allow higher common-depth-point multiplicity and provide better noise cancellation. Exact field-recording configurations should be established after sufficient noise analysis to determine the optimum source and geophone configuration for best noise cancellation.

Seismic-reflection data should be capable of providing very high resolution of the subsurface. For an interbed 15 m thick and an interval velocity of 3,000 m/s, a seismic pulse that is 0.01 s wide would be desirable. For such reflectors, frequencies of at least 100 Hz would be desired. Burial of the geophones would optimize ground coupling, and high-frequency seismic data would be detected.

Borehole Geophysics

All of the surface seismic profiling and vertical seismic profiling could be effectively tied to the geology by logging wells drilled to the depth of interest.

CONCLUSIONS

From this study, we obtained the following results and conclusions:

1. Analysis of approximately 50 km of conventional seismic-reflection data using surface arrays and both impulsive and controlled sources indicates that the potential exists for mapping shallow, high-acoustic contrast, isolated thin beds in a homogeneous salt.
2. Computer ray-trace modeling has aided in the identification of frequency and spatial-resolution limitations that are present in most petroleum seismic data. For more detailed mapping of very thin (5-70 m), intensely folded interbeds at depths of less than 750 m, frequencies on the order of 500 Hz and surface-spread lengths of less than 350 m are recommended. Furthermore, considerations should be given to burial of both the source and receiver arrays in order to attenuate surface-related noise.
3. Correlation of the seismic-reflection data with available well data and surface geology in the area of the salt-cored anticlines in the Paradox Basin of southeastern Utah confirms a complex, structurally initiated, basement-fault-controlled salt diapir. Its upward flow was influenced by contemporaneous deposition of Permian continental clastic sediments in the adjacent synclines, which were formed by removal of the salt. Complex inhomogeneities

near the surface, caused by solution of these diapirs near the crests, are responsible for distortion of the seismic response.

4. Evidence exists that thin interbeds of anhydrite, dolomite, and black shale are mappable, either as anomalous amplitudes due to focusing at depth or as short, discontinuous segments. Computer modeling of folded thin beds in salt confirms both of these as possible causes for the intrasalt seismic response observed on the seismic-reflection profiles.

5. The following refinements of existing seismic-reflection methods and their integration with other geophysical techniques should allow more direct identification of the interbeds in salt: vertical seismic profiling and a shallow, short-offset, high-multiplicity, high-frequency, seismic-reflection survey.

REFERENCES CITED

- Cater, F. W., 1970, Geology of the salt anticline region in southwestern Colorado, with a section on Stratigraphy, by F. W. Cater and L. C. Craig: U.S. Geological Survey Professional Paper 637, 80 p. [1971].
- Gal'perin, E. I., trans. by A. J. Hermont, ed. by J. E. White, 1974, Vertical seismic profiling: Society of Exploratory Geophysicists Special Publication 12, 270 p. [Originally published as "Vertikal'noe seismicheskoe profilirovanie," Moskva, Nedra, 1971.]
- Gard, L. M., 1976, Geology of the north end of the Salt Valley anticline, Grand County, Utah: U.S. Geological Survey Open-File Report 76-303, 35 p.
- Hite, R. J., and Lohman, S. W., 1973, Geologic appraisal of Paradox Basin salt deposits for waste emplacement: U.S. Geological Survey Open-File Report, 75 p.
- Kupfer, D. H., 1968, Relationship of internal to external structure of salt domes, in Diapirism and diapirs--A symposium: American Association of Petroleum Geologists Memoir 8, p. 79-89.
- LeFond, S. J., 1969, Handbook of world salt resources: New York, Plenum Press (monographs in geoscience), 384 p.
- Wuenschel, P. C., 1976, The vertical array in reflection seismology--some experimental studies: Geophysics, v. 41, no. 2, p. 219-232.